Northumbria Research Link

www.northumbria.ac.uk/nrl

northumbria
UNIVERSITY NEWCASTLE

Non-Data Aided Rician Parameters Estimation in Temporal Fading Channel With 3 DoFs Gaussian Mixture Model

QILONG ZHANG[1], GUOBAO LU[1], (Student Member, IEEE), WUXIONG ZHANG[2], (Member, IEEE), FEI SHEN[2], (Member, IEEE), XUEWU DAI[3], (Member, IEEE), JIANBIN JIAO[1], (Member, IEEE), AND FEI QIN[1,4], (Member, IEEE)

[1]School of Electronic and Electrical Communication Engineering, University of Chinese Academy of Sciences, Beijing 100049, China
[2]Shanghai Institute of Microsystem and Information Technology, Chinese Academy of Sciences, Shanghai 200050, China
[3]Department of Mathematics, Physics and Electrical Engineering, Northumbria University, New Castle NE1 8ST, U.K.
[4]Key Laboratory of Information Technology for Autonomous Underwater Vehicles, Chinese Academy of Sciences, Beijing 100190, China

Corresponding author: Fei Qin (fqin1982@ucas.ac.cn)

ABSTRACT Rician distribution has been widely utilized to describe wireless fading channel. In the non-stationary temporal fading channel like industrial scenarios, both the specular and scattered components of the multi-path fading channel will be time varying. As a result, the online estimation of Rician parameters is necessary to provide stable wireless service. The traditional estimation approaches of Rician parameters are designed for channel measurement usage and therefore have to work in the data-aided mode for online estimation with modulated I/Q samples. To solve this problem, some non-data-aided algorithms have been proposed in recent years, but only valid in specific scenarios. In this paper, we formulate the estimation of Rician parameters from modulated I/Q samples as a two-dimensional Gaussian mixture model to provide a general non-data-aided Rician parameter estimation method. By involving *a priori* information of modulation scheme and the motivation of optimized gradient searching, the independent parameters in the maximum likelihood estimation can be significantly decreased to three, which leads to fast convergence of the modified expectation–maximization algorithm with high accuracy. The combination of these modifications has been finally formulated as a Rician mixture model. The numerical results and field measurements illustrate the feasibility of this methodology.

INDEX TERMS Rician distribution, maximum likelihood estimation, non-data aided, Gaussian mixture model.

I. INTRODUCTION

The wireless channel of fixed wireless link in the industrial scenario has been investigated over decades [1]–[9]. Obvious, the massive metal surfaces in industrial scenarios will lead to complex fading channel models due to the multi-path effect. In an ideal fixed wireless link, although the delay and attenuation of signals from multiple paths still vary according to

The associate editor coordinating the review of this manuscript and approving it for publication was Xiao-Sheng Si.

different paths, the combination of these signals will be static over time. However, most industrial environments are non-ideal: the nearby moving objects will generate dynamic paths, which will also perturb the stationary scattered paths. As a result, both the specular and scattered power of the received signal will be time-varying with specific pattern rooted in the arbitrary mobility pattern of moving objects [9]. Such effect has been observed and termed as the non-stationary temporal fading [2], [4], [6], [7], [9]. In the temporal fading channel, the envelop of the received signal will still follow the Rician
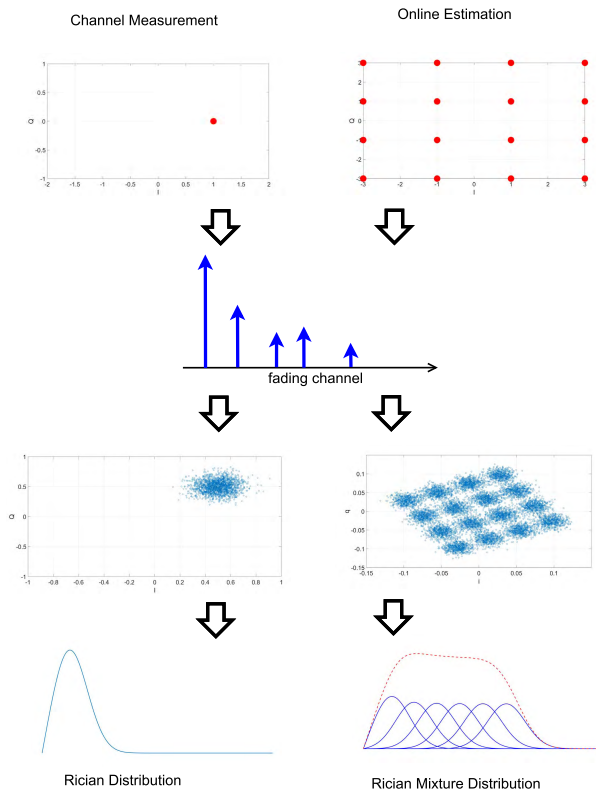
FIGURE 1. The problem in Rician parameter estimation with modulated IQ samples.

distribution but with time varying parameters of *s* and σ due to the essential varying nature of both specular and scattered components. Then, the internal thermal noise won't be the only source of causing transmission error, which is better represented by the famous Rician *K* factor, i.e., $K = s^2/2\sigma^2$. If consider the time varying nature of the temporal fading channel, these Rician parameters must be on-line updated from time to time to obtain an accurate link quality metric. Otherwise, the transceiver may take wrong actions due to inaccurate link quality information which may result in serious consequence. For example, in the wireless closed-loop control system [10], [11], the wireless networks must provide strict constraint services on reliability [12] and timing (e.g. delays) [13]. Otherwise, the closed-loop control system may become unstable resulting in the unplanned shutdown, equipment damage, safety risk and economic loss. Nonetheless, an online accurate estimation of Rician parameters of the temporal fading channel is the key to guarantee reliable services [14], [15].

The estimation of Rician parameters is of considerable interest. The earlier approaches [16]–[18] only work on the envelop of the received signal from the fading channel and rely on the moment based estimation method. The coming after approaches [19]–[21] choose to utilize both the amplitude and phase information from I/Q streams through Maximum Likelihood Estimation (MLE) method to increase reliability and accuracy. However, these approaches are usu-

ally designed for channel measurement of static or stationary fading channel, i.e., the I/Q stream are utilized only for channel measurement. Nonetheless, these algorithms fail to be directly ported from channel measurement system into online channel estimation system, since the existence of modulated symbols will discretize the received cluster in constellations, as shown in Fig.1. Then both the moment based and phase based methods cannot be directly applied but have to be data-aided to cancel the self-interference of modulated signals [22], hence fail to utilize massive modulated I/Q samples. Against this limitation, the Auto-Correlation Function (ACF) has been adopted [22] to avoid the data aided requirement, which, however, cannot be applied within M-ary Phase Shift Keying (M-PSK) scenarios due to the null ACF. The most recent work in [23] and [24] employ the fourth order cross moment statistic to avoid the data aided constraint, which can only work in the specified Single Input Multiple Output (SIMO) scenarios, i.e. not applicable in common single input single output scenarios especially the industrial scenario.

As demonstrated in our previous work [9], such a Rician parameter based online estimator from modulated I/Q stream can significantly increase the link quality estimation performance in the non-stationary industrial fading channel. If aware that some recently released Commercial off-the-shelf (COTS) wireless transceivers (e.g., Atmel AT86RF215 [25]) have open the I/Q stream interface, the user-defined link quality estimator can be deployed in the COTS transceiver to gain better link capacity and reliability. In this paper, we propose a novel non-data aided approach to directly estimate Rician parameters from modulated I/Q streams. As revealed by Fig.1, the modulated I/Q stream after a Rician fading channel will form two dimensional Gaussian clusters in the received constellations, the number of which is decided by the modulation order. In the data aided model, all the deviations caused by the modulation can be self-cancelled and the residue deviations will only be contributed by the fading channel. In the scenario without data aiding, it is straightforward to treat the received constellations as a classical two dimensional Gaussian Mixture Model (GMM), which can be solved by the famous Expectation-Maximization (EM) algorithm. The estimated results can be utilized to cancel the modulation interference. However, this method will suffer from the long converging problem and fail to be utilized in the online estimation. The proposed method in this paper is based on the fact that although the exact modulated symbol sequences are unknown, the modulation scheme can be assumed as *a priori* information. This essential fact can be utilized to approximate the optimized gradient search in the EM algorithm, so that not only the converge process can be accelerated but also the converged accuracy can be improved. This problem has been modeled as a 3 Degrees of Freedom (DoFs) GMM algorithm or termed as the Rician Mixture Model (RMM) algorithm according to its mathematical form.

The rest of this paper is outlined as follows: section II provides the problem formulation. The design of 3 DoFs GMM based estimation method is presented in section III.

Experiments from numerical simulation and industrial sites are utilized to validate the proposed algorithm in section IV, followed by the conclusion in section V.

II. PROBLEM FORMULATION

The narrowband complex baseband representation of Rician fading channel can be modeled by [17]:

$$h(t) = \sqrt{\frac{K\Omega}{K+1}} h_{sp}(t) + \sqrt{\frac{\Omega}{K+1}} h_{sc}(t), \quad (1)$$

where the first item $h_{sp}(t)$ is termed as specular component contributed by the Line of Sight (LOS) path or other strong dynamic path, while the second item $h_{sc}(t)$ is termed as scattered component representing all other scattered paths. The parameter Ω represents the average power of the received signal, while K represents the ratio between specular power s^2 and scattered power $2\sigma^2$. In this context, the received envelop after fading channel will follow the Rician distribution:

$$f_R(r_n|s, \sigma) = \frac{r_n}{\sigma^2} \exp\left(-\frac{r_n^2 + s^2}{2\sigma^2}\right) I_0\left(\frac{s \cdot r_n}{\sigma^2}\right). \quad (2)$$

where r_n is the envelope of the nth sample.

It is easy to notice the existence of a zero order Bessel function $I_0(\cdot)$. As a result, the estimation of K with moment statistics usually requires iterative based algorithm [16]. Another choice [18] is to estimate Rician parameters through higher order moment statistics to obtain the closed-form solution, which may require large samples and suffer from the loss of accuracy and reliability.

As the received I/Q streams can be utilized for estimation through the transceiver interface, then it is possible to utilize both amplitude and phase to obtain a reliable estimation of Rician parameters. The Rician distribution is derived from the assumption that the scattered components are independently distributed in both I and Q dimensions. According to the central limit theorem, it is reasonable to assume that they all follow the Gaussian distribution. The joint distribution of I and Q can be written as:

$$f_{I,Q}(r_{i,n}, r_{q,n}|\mu_i, \mu_q, \sigma_i, \sigma_q)$$
$$= \frac{1}{\sqrt{2\pi\sigma_i^2}} exp\left(-\frac{(r_{i,n} - \mu_i)^2}{2\sigma_i^2}\right) \frac{1}{\sqrt{2\pi\sigma_q^2}} exp\left(-\frac{(r_{q,n} - \mu_q)^2}{2\sigma_q^2}\right), \quad (3)$$

where μ_i and μ_q are contributed by the specular component, σ_i and σ_q are contributed by all the scattered components, respectively.

With simple geometrical derivation and a priori information of fading channel, the new variable of r, ϕ, and ϕ_0 can be introduced to map received signal into polar coordinates:

$$s^2 = \mu_i^2 + \mu_q^2$$
$$r_n^2 = r_{i,n}^2 + r_{q,n}^2$$
$$\phi_0 = arctan\left(\frac{\mu_i}{\mu_q}\right)$$

$$\phi_n = arctan\left(\frac{r_{i,n}}{r_{q,n}}\right), \quad (4)$$

where r is the envelope of the received signal, ϕ is the phase of received signal (i.e., calculated from the I/Q stream), especially ϕ_0 is the phase variation caused by the specular components in the fading model. The joint Power Density Function (PDF) of the envelope and phase can be formulated with the help of Jacobian determinant:

$$f_{R,\Phi}(r_n, \phi_n|s, \sigma, \phi_0)$$
$$= \frac{r_n}{2\pi\sigma^2} \exp\left(-\frac{r_n^2 + s^2 - 2r_n s \cos(\phi_n - \phi_0)}{2\sigma^2}\right). \quad (5)$$

With further integration over ϕ, equation (5) could be degraded to equation (2). Without any doubt, the joint PDF will provide more information with introduced phase item. As shown in [21], following the classical concave method, the log-likelihood of equation (5) can be simply obtained as:

$$\ln f_{R,\Phi}(r_n, \phi_n|s, \sigma, \phi_0)$$
$$= \frac{s}{\sigma^2} \sum_{n=1}^{N} r_n \cos(\phi_n - \phi_0)$$
$$+ \sum_{n=1}^{N} \ln r_n - \frac{1}{2\sigma^2} \sum_{n=1}^{N} r_n^2 - \frac{Ns^2}{2\sigma^2} - N \ln\left(2\pi\sigma^2\right). \quad (6)$$

where N is the number of samples.

Then, the MLE estimation of Rician parameters from received I/Q streams can be written as:

$$\hat{s} = \frac{1}{N} \sum_{n=1}^{N} r_n \cos(\phi_n - \phi_0)$$
$$2\hat{\sigma}^2 = \frac{1}{N} \sum_{n=1}^{N} r_n^2 - \hat{s}^2$$
$$\hat{\phi}_0 = \arctan\left[\frac{\sum_{n=1}^{N} r_n \sin(\phi_n)}{\sum_{n=1}^{N} r_n \cos(\phi_n)}\right]. \quad (7)$$

Simply applying $K = s^2/2\sigma^2$ will lead to a high accuracy and reliable estimation of Rician K factor due to the utilization of additional phase information. Be aware that in the non-stationary fading channel, all parameters are time varying and should be rewritten as a function with variable of time. Yet, the estimation of Rician K factors requires the online fashion. Without any doubt, the above algorithm can only work with non-modulated signal or require a priori information on the transmitted symbols, which has been shown in the upper area of Fig.1. If take M-PSK as an example scenario, equation (5) should be rewritten as:

$$f_{R,\Phi}(r_n, \phi_n)$$
$$= \frac{r_n}{2\pi\sigma^2} \exp\left(-\frac{r_n^2 + s^2 - 2r_n s \cos(\phi_n - \phi_0 - \phi_{s,n})}{2\sigma^2}\right), \quad (8)$$

where $\phi_{s,n}$ is the modulation phase for each symbol. For the QAM based modulation, additional $a_{s,n}$ denoting the

modulation amplitude for each symbol should be further involved. If with the known transmitted symbol information, i.e. Data Aided model, $a_{s,n}$ and $\phi_{s,n}$ could be self-cancelled, the problem will be a standard Rician parameter identification problem. But the number of symbols with known information is usually limited, e.g. preamble or pilot symbols. As a result, all the rest modulated symbols with $a_{s,n} \neq 1$ and $\phi_{s,n} \neq 0$ cannot be utilized to estimate Rician parameters with the classical MLE algorithm, which may cause a higher estimation variation. Be aware that in this case even the moment based method is unable to estimate the Rician parameters due to the multiple levels of modulated amplitude, which has been shown in the lower area of Fig.1. As discussed, a general algorithm to utilize the massive modulated signal to estimate Rician parameters is still an open and challenging problem.

III. 3 DoF GAUSSIAN MIXTURE MODEL

As shown in equation (8), the current problem is to identify distribution parameters from modulated symbol streams, where $a_{s,n}$ & $\phi_{s,n}$ will be discretized with different modulation schemes. Take the popular Quadrature Phase Shift Keying (QPSK) modulation scheme utilized in IEEE 802.15.4 system as an example. This can be intuitively understood as a single cluster decentralized into four clusters, which are equally separated in a phase circle of constellations. Similarly, other modulation schemes will also form different regular cluster pattern in the constellations, which can be modeled as a mixed two dimensional Gaussian distribution:

$$
\begin{aligned}
&f_{I,Q}(r_{i,n}, r_{q,n}|\mu_{i,m}, \mu_{q,m}, \sigma_{i,m}, \sigma_{q,m}) \\
&= \sum_{m=1}^{M} \omega_m \frac{1}{\sqrt{2\pi\sigma_{i,m}^2}} exp(-\frac{(r_{i,n} - \mu_{i,m})^2}{2\sigma_{i,m}^2}) \\
&\quad \times \frac{1}{\sqrt{2\pi\sigma_{q,m}^2}} exp(-\frac{(r_{q,n} - \mu_{q,m})^2}{2\sigma_{q,m}^2}),
\end{aligned}
\tag{9}
$$

where M is the modulation order, e.g., 4 for QPSK, 8 for 8-PSK, and 16 for 16-QAM; $\mu_{i,m}$ & $\mu_{q,m}$ are the coordinates of each cluster center, decided by both the fading effect and modulation scheme; similarly, $\sigma_{i,m}$ & $\sigma_{q,m}$ represent the deviation degree caused by the fading effect; and finally ω_m refers to the weight for each cluster. To be brief, equation (9) can be rewritten with the general two dimensional Gaussian function:

$$
f_{I,Q}(x_n|\mu, \Sigma)) = \sum_{m=1}^{M} \omega_m G(x_n|\mu_m, \Sigma_m),
\tag{10}
$$

where $G(\cdot)$ denotes the PDF of two dimensional Gaussian distribution. $x_n = [r_{i,n}, r_{q,n}]^T$ describes the received symbol, $\mu_m = [\mu_{i,m}, \mu_{q,m}]^T$ describes the center of each cluster with index m, and $\Sigma_m = \begin{bmatrix} \sigma_{i,m} & COV_{I,Q} \\ COV_{Q,I} & \sigma_{q,m} \end{bmatrix}$ describes the variation of each cluster with index m. Be aware, $COV_{I,Q}$ and $COV_{Q,I}$ are the covariances of the two dimensional Gaussian distribution, and are in fact 0 with known constraint of Rician

distribution. μ and Σ refer to the sets of μ_m and Σ_m respectively. Consequently, the probability of the current symbol belong to the mth cluster can be modeled as:

$$
p_{n,m} = \frac{\omega_m G(x_n|\mu_m, \Sigma_m)}{\sum_{j=1}^{M} \omega_j G(x_n|\mu_j, \Sigma_j)},
\tag{11}
$$

Nonetheless, the current form of problem can be treated as a classical GMM and solved by the famous EM solution, which iteratively converges to the optimized estimations of $\hat{\mu_m}$, $\hat{\Sigma_m}$ and $\hat{\omega_m}$. Be aware that μ_m and Σ_m are in fact large number of parameters: the size of μ_m is 2 for each cluster, while the size of Σ_m is 4 for each cluster. Further considering one more parameter of ω_m for each cluster, there will be $2 + 4 + 1 = 7$ parameters waiting for estimation of each cluster. Then, the overall number of parameters waiting for estimation will be $7M$ in total, as there are M clusters. Obviously, the converge process will be correlated with the modulation order M, e.g. the larger the M is, the longer and harder the converge process will be. Consequently, long converge process will cost high computation resources and time, which can not be afforded in the online estimation algorithm with time constraints. This is why we decide not to simply adopt the classical EM solution.

Without any doubt, some *a priori* information from modulation scheme can be utilized as constraints for this mixed Gaussian distribution, which can significantly ease the solving complexity. Normally, the transmitted number of symbols will be much larger than the modulation order, which can lead to the constraints of the equal weights of $\omega_m = \frac{1}{M}$ for each cluster. As a result, equation (11) can be rewritten as:

$$
p_{n,m} = \frac{G(x_n|\mu_m, \Sigma_m)}{\sum_{j=1}^{M} G(x_n|\mu_j, \Sigma_j)}.
\tag{12}
$$

The log-likelihood function can be written as:

$$
\ln f_{I,Q}(x_n|\mu, \Sigma) = \sum_{n=1}^{N} \ln \sum_{m=1}^{M} \frac{1}{M} G(x_n|\mu_m, \Sigma_m),
\tag{13}
$$

As expected, even with simplified ω_m, the above equation cannot be analytically solved. However, by applying the Jensen's inequality, the lower bound of the above equation can be obtained as:

$$
\ln f_{I,Q}(x_n|\mu, \Sigma) \geq \sum_{n=1}^{N} \sum_{m=1}^{M} p_{n,m} \ln \frac{G(x_n|\mu_m, \Sigma_m)}{M \cdot p_{n,m}}.
\tag{14}
$$

Now, the problem can be equalized to the Max-Min problem in the M-step, and the iterative estimation of $p_{n,m}$ in the E-step. In the classical EM solution, the MLE solution will be utilized in the M-step to maximize the lower bound of likelihood function. As discussed earlier in this section, it is reasonable to utilize the *a priori* information of modulation scheme in this scenario. If treat the MLE algorithm as the analytical optimized solution of convex coordinates, then the EM solution is an equalized form of the gradient search problem with pseudo maximized solution in each iterative cycle.
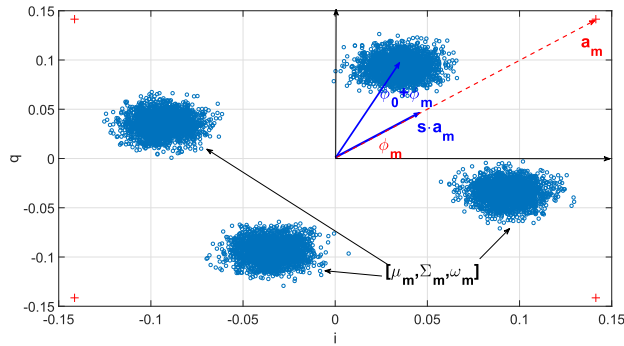
FIGURE 2. The scheme of 3 DoFs MLE estimation of Gaussian Mixture Model.

Obviously, *a priori* information of the modulation scheme can be utilized to guild the optimized gradient searching.

Similar to ω_m, the modulation scheme is also a utilizable *a priori* information. Considering a transceiver pair over fading channel, once the modulation scheme was negotiated by two transceivers, the pattern of transmitted constellations will be fixed, which will then be scaled in the amplitude, rotated in phase, and resulted in the received constellations. As shown in Fig.2, although there are $7M$ explicit parameters in equation (9), the essential DoFs are only 3 with known modulation scheme. This is due to the fact that the relative distances and angles among constellations are fixed due to modulation scheme. The fading channel will only cause all the constellations, an indivisible whole, to scale in amplitude s, to rotate in angle ϕ_0, and to scatter in the variation of amplitude σ. For example, if the constellation in the first quadrant has been rotated with ϕ_0, all the other three constellations in different quadrant will also suffer from the same ϕ_0 rather than other angle. It is not likely all the $7M$ parameters will change independently, instead they have been essentially correlated with 3 DoFs system. In other words, the optimized direction in the gradient search can only occur in $\vec{s}$, $\vec{\sigma}$ and $\vec{\phi_0}$.

After some algebra, equation (9) could be rewritten in the mixed Rician fashion and termed as RMM:

$$f_{R,\Phi}(r_n, \phi_n|s, \sigma, \phi_0) = \sum_{m=1}^{M} \frac{f_m(r_n, \phi_n|s, \sigma, \phi_0, a_m, \phi_m)}{M} \quad (15)$$

where s, σ, and ϕ_0 are the fading channel related parameters; a_m and ϕ_m have been treated as the known modulation parameters for the mth transmitted constellation. The PDF $f_m(\cdot)$ for each cluster can be simply defined with modified equation (5):

$$f_m(r_n, \phi_n|s, \sigma, \phi_0, a_m, \phi_m)$$
$$= \frac{r_n}{2\pi\sigma^2}$$
$$\times \exp\left(-\frac{r_n^2 + a_m s^2 - 2a_m r_n s \cos(\phi_n - \phi_0 - \phi_m)}{2\sigma^2}\right), \quad (16)$$

It was expected that the current form of RMM will regulate the gradient search only in s, σ and ϕ_0. By applying equation (15) (16) into equation (14) to instead $f_{IQ(\cdot)}$ and $G(\cdot)$ respectively. Following the derivation in equation (6), the pseudo-MLE of parameters in the M-step can be easily obtained with respect to s, σ and ϕ_0.

$$\hat{s} = \frac{1}{N}\sum_{n=1}^{N}\sum_{m=1}^{M} p_{n,m}\frac{r_n \cos(\phi_n - \phi_0 - \phi_m)}{a_m}$$

$$2\hat{\sigma}^2 = \frac{1}{N}\sum_{n=1}^{N}\sum_{m=1}^{M} p_{n,m}[r_n^2 - (\hat{s}\cdot a_m)^2]$$

$$\hat{\phi_0} = arctan\left[\frac{\sum_{n=1}^{N}\sum_{m=1}^{M} p_{n,m}r_n \sin(\phi_n - \phi_m)}{\sum_{n=1}^{N}\sum_{m=1}^{M} p_{n,m}r_n \cos(\phi_n - \phi_m)}\right]. \quad (17)$$

And equation (12) could still be utilized in the E-step. It is easy to prove that such a solution is compatible with the classical EM solution with 2 dimension GMM, but with additional regulation that all the fine tune in θ (parameters) should be mapped to $\vec{s}$ and $\vec{\phi_0}$. This is due to the fact that the essential improvement is the optimized gradient search with known information of modulation scheme.

Similar to many other GMM-like algorithms, the performance of the proposed optimized gradient search based RMM is closely related to the initial configurations. In other words, it can be further increased with K-means pre-processing, which can provide a rough estimation as the inputs.

IV. EXPERIMENT VALIDATION
A. NUMERICAL RESULTS
The performance of the proposed methodology is first evaluated by numerical experiments implemented in Maltab. Compared to fields experiments presented in subsection B, the main benefit of numerical experiment is the known true values of Rician parameters s, σ and their variation K. In each numerical experiment, the preset Rician parameters will be utilized to generate a stream of I/Q samples last 127byte*8bit*16chip. These numbers are set according to the most popular IEEE 802.15.4 transceiver in the wireless industrial applications [26]. The generated I/Q stream will be processed by four chosen estimation algorithms, including the Data Aided mode with all known symbols (DA-all), the Data Aided mode with only limited number of known pilot symbols (DA-pilot), the classical GMM based non-data aided mode (GMM), and the proposed 3 DoFs GMM mode or briefly referred as its formulation Rician Mixture model (RMM) in the following section. The estimated result will be compared with the known ground truth to evaluate the performance of four chosen method.

The intuitive results of how the GMM/RMM estimation can fit the faded symbols have been firstly provided in Fig.3. In Fig.3 (a) the classical GMM algorithm provided by Matlab has been applied to the I/Q streams in the QPSK scenario. In Fig.3 (b) the proposed RMM methodology has been applied to the same streams. The K factor for this scenario
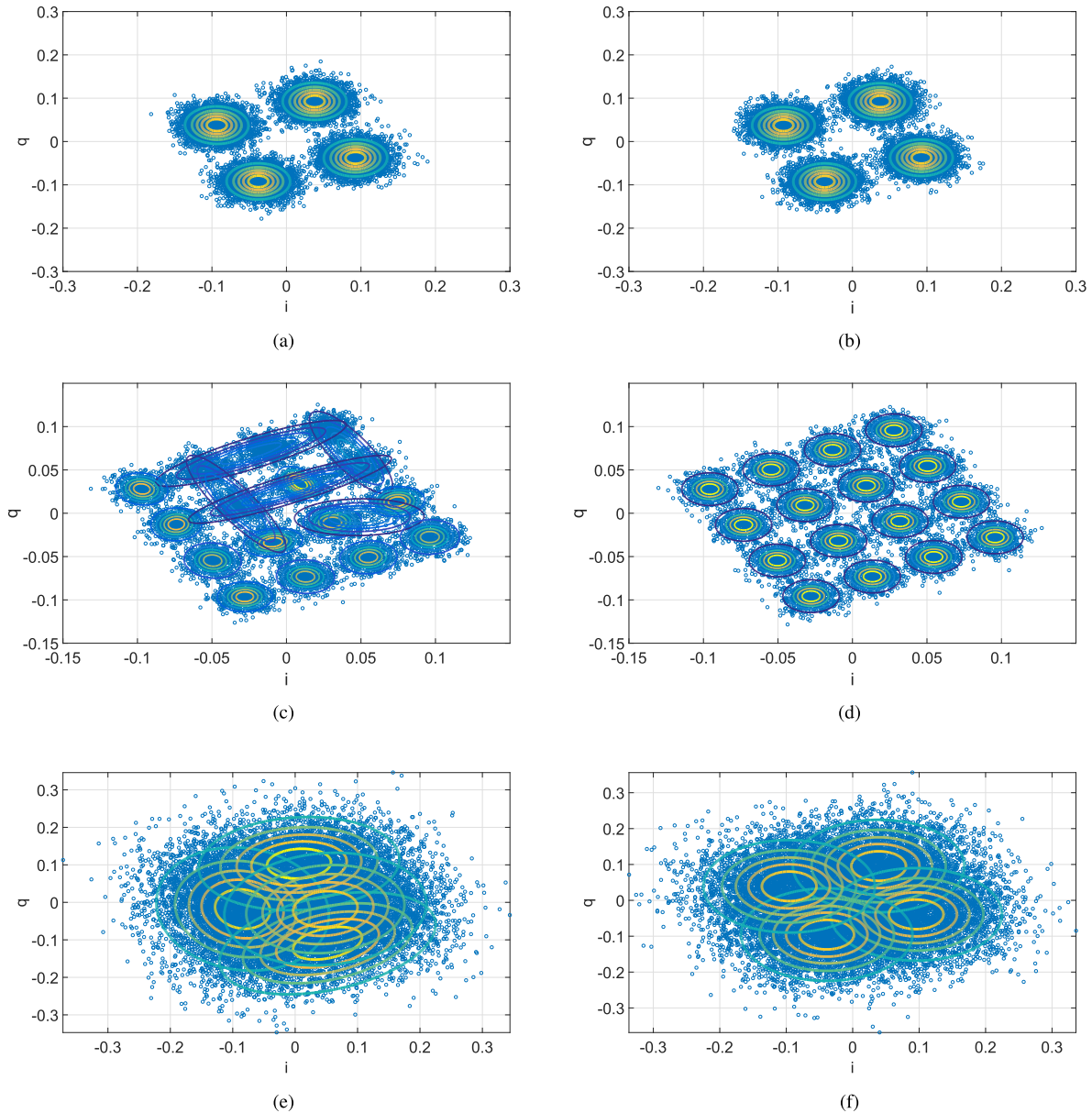
FIGURE 3. The typical estimated results: (a) QPSK with GMM in ideal scenario; (b) QPSK with RMM in ideal scenario; (c) 16-QAM with GMM in ideal scenario; (d) 16-QAM with RMM in ideal scenario; (e) QPSK with GMM in challenge scenario; (f) QPSK with RMM in challenge scenario.

has been set to be 10, which contributes an easy problem for GMM estimation as the clusters are far away from each other. The received symbols have been shown with the scattered plots in the figure, while the estimated results have been shown in the contour form of the two dimensional Gaussian distribution. Clearly, both methods have achieved almost perfect fitting performance. It will also be clear that the situation will be tougher in the 16-QAM scenario as shown in Fig.3 (c) and Fig.3 (d) with same configuration. As expected the classical GMM method failed to fit all 16 clusters, since 5 in 16 potential clusters have been wrongly estimated. This is due to the increased DoFs, i.e. from $7 \times 4 = 28$ to $7 \times 16 = 112$. As a result, the risk of convergence with false results will

be increased. Due to the similar reason, as the DoFs has been decreased from $7 \times 16 = 112$ to 3 in the proposed RMM method, the estimation result is still perfect to fit all 16 clusters. In Fig.3 (e) and Fig.3 (f), the configuration of K has been significantly decreased to only 1, which leads to significantly overlapped constellations. Again, the classical GMM method failed to converge to the known ground truth, while the proposed RMM method still successfully converged even in this challenging scenario.

After the intuitive results, the quantitative performance will be presented and discussed. Fig.4 shows the Root Mean Square Error (RMSE) results of all four evaluated algorithms in the QPSK scenario. The RMSE calculations follow the
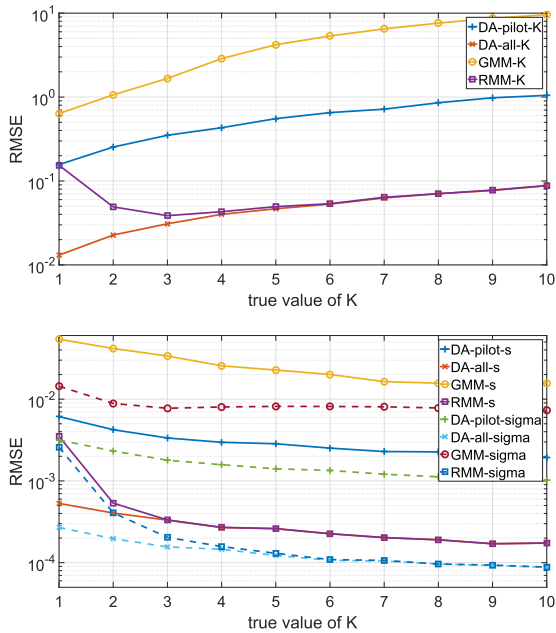
FIGURE 4. The RMSE performance with different K in QPSK scenario.

FIGURE 5. The RMSE performance with different ϕ_0 in QPSK scenario.

standard algorithm as shown in equation(18):

$$RMSE = \sqrt{\frac{1}{R}\sum_{r=1}^{R}(\hat{K}_r - K_r)^2} \qquad (18)$$

where R is the repeated numbers of each experiment. In the experiments, K will be increased from 1 to 10. In the DA-all mode, all the received I/Q samples are assumed with known symbol information. Obviously, this is not a realistic mode, as it contains no information and can only be utilized to estimate the channel status. But there are other efficient candidates if all the transmitted bandwidth can be invested in the channel estimation. Yet, this method was chosen to act as a rough lower bound of the estimation error for the proposed algorithms[1]. In the DA-pilot mode, around 1% I/Q samples are assumed with known symbol information, these symbols are usually termed as pilot symbols in the transceiver design, which contribute to the brief name of DA-pilot.

In Fig.4, the DA-all method performs the best achieving only 0.013 RMSE in the estimation of K with the configuration of $K = 1$, and 0.087 RMSE with $K = 10$. Obviously, the GMM method performs the worst showing similar trends but higher error, i.e. 0.63 RMSE with $K = 1$, and 9.57 RMSE with $K = 10$. It is interesting to notice that the DA-pilot method shows similar but slightly better performance than the GMM method, increasing the RMSE from 0.15 to 1.04, which means that the GMM method costs much more computation resources to converge to a worse result. This may explain why there is no previous published work attempting to utilize GMM in Rician parameter estimation. On the

other side, the proposed RMM method has shown the trends approximating the lower bound (DA-all), i.e. from 0.15 to 0.08 with turning point of 0.038 when $K = 3$. The slightly worse performance with small K is reasonable as the clusters in constellation will involve large overlap, which increases not only the difficulty of convergence but also the accuracy of estimation results. After $K = 3$, the proposed RMM method quickly converges to almost the similar performance of DA-all.

There is a logical paradox here, that with the increased K, the difficulty of estimation will be eased as the cluster will be far away from each other. Normally, the RMSE of estimation results should be decreased in this scenario but not for the estimated K in the experiments. This can be understand, if recall the fact that s and σ are the directly estimated parameters, which will be further utilized to calculate K. Now, if refer to the lower sub-figure of Fig.4, all the RMSE performances of estimated s and σ are decreasing with increasing K. However, the estimation error of σ will be significantly amplified in the calculation of $K = s^2/2\sigma^2$, which finally leads to the increasing RMSE of K.

Fig.5 provides the RMSE with different ϕ_0 in the QPSK scenario, where the K factor has been set as 1, i.e. a challenge scenario. As expected, the estimation error is stable for all four validated methods. The DA-all method shows a stationary pattern around 0.05, which is the best accuracy. The proposed RMM method shows the second lowest error around 0.04. The other two candidates show much worse performance around 0.61 and 5.37 RMSE for DA-pilot and GMM respectively. These results reveal two facts: firstly, all four methods are not sensitive to the specular path delay, i.e. the variation of ϕ_0; secondly, the proposed RMM method is still the best candidate approaching the 'lower bound' DA-all.

---

[1]We are aware of the I.I.D assumption, the Lag pre-process in [22] can be further employed to satisfy such assumption and increase the estimation performance.
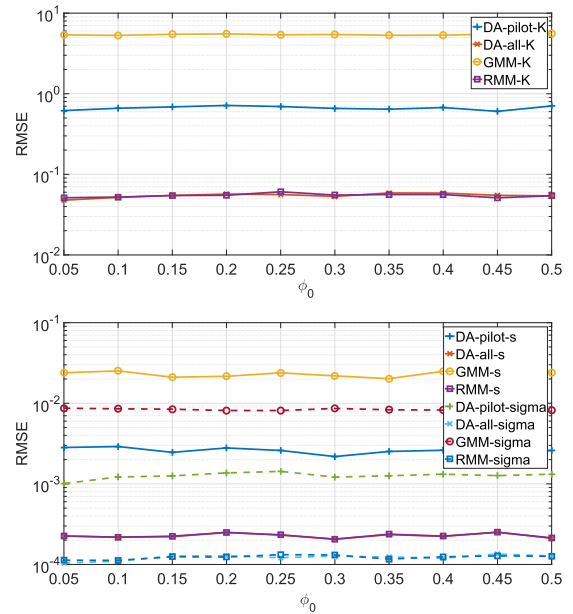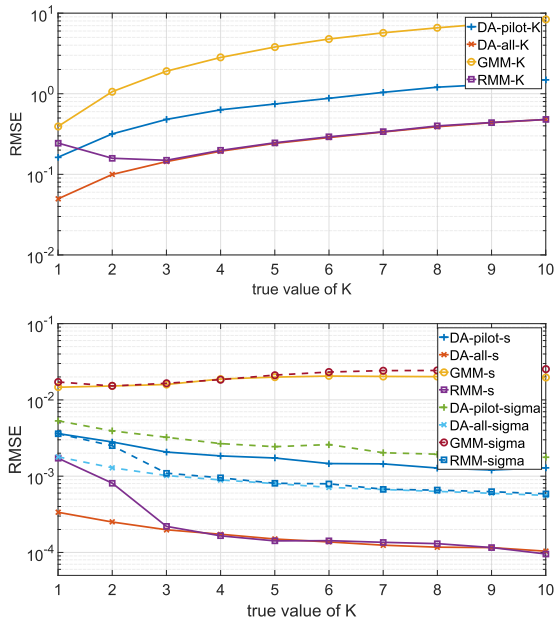
FIGURE 6. The RMSE performance with different K in 16-QAM scenario.

FIGURE 8. The convergence with different K in 16-QAM scenario.

Fig.6 provides the RMSE with different K in the 16-QAM scenario. The performance is very similar to the results shown in Fig.4, except the slightly increased challenge due to the deeper modulation order as shown in Fig.3. The RMSE performance of K in DA-all method increases from 0.04 to 0.47 with K increasing from 1 to 10. The almost similar performance has been achieved by RMM with RMSE increasing from 0.24 to 0.47 with turning point of 0.14 when $K = 3$. At the same time, the DA-pilot method shows RMSE increasing from 0.16 to 1.49, while the GMM method increasing from 0.39 to 8.36. These results confirm the performance rank still applicable in the 16-QAM scenario, but with slightly worse performance than the QPSK scenario. It should be noticed that the RMSE performances of s and σ in GMM method fail to decrease as other methods, which hints the fact that GMM may usually hard to converge to the ground truth in the 16-QAM scenario. As Fig.5 already demonstrated
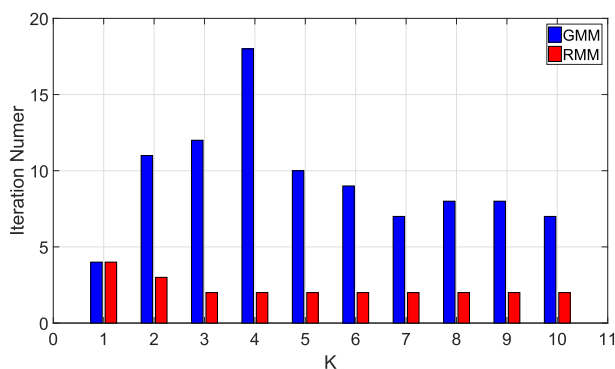
the insensitive nature with ϕ_0, the similar experiment was not shown for 16-QAM.

Given the estimation accuracy, the complexity of all four methods will be evaluated in Fig.7 and Fig.8. Without any doubt, the time computation cost is as important as the estimation accuracy to decide whether the proposed method can be employed in the intention application. To achieve this objective, the number of iteration cycles before convergence has been chosen as the performance metric. The converge condition have been set to 0.1%. Also as the DA-all and DA-pilot are not iteration based, the number of iteration cycles are assumed as 1 and not drawn in the figures. Be aware that similar MLE solution has been utilized in all four methods, so the computational cost for each iteration cycle can be roughly assumed to be the same. The QPSK scenario has been provided in Fig.7 first. The performance of RMM shows the clear and reasonable pattern, 4 iteration cycles in the most challenging scenario with $K = 1$ and quickly decreases to only 2 iteration cycles in almost all other scenarios. As already mentioned, in each iteration cycle, a standard MLE algorithm will be deployed with linear complexity, the overall computational cost for RMM can be simply afforded in most applications[2]. For the GMM, it is clear that GMM costs more iteration cycles with an average number around 9. It is interesting to notice that the maximum cost of GMM appeared at $K = 4$. If refer to Fig.3, clusters will be heavy overlap with each other with small K. In this scenario, there could be many near optimal solutions existed to fit such overlapped constellations. As a result, the GMM method may easily converges to one of the near optimal solution very fast instead being able to find the ground truth. With increasing K, the clusters will centrifuge with each other, and the ground truth will become significant in the solution space. As a result, the GMM method now has the possibility to approach the ground truth with longer searching iterations shown in Fig.7.

FIGURE 7. The convergence with different K in QPSK scenario.

[2]In this paper, the algorithms are implemented in Maltab running on an Intel Xeon E5-2603 CPU @ 1.6GHz, which provide a time cost around 28*ms* per iteration cycle. It should noted that the actual time cost can be hundreds or even thousands smaller in a hardware implementation with simple optimization of the code, which can be employed to obtain a rough estimation of time costs.

The 16-QAM scenario has been provided in Fig.8. As expected, both RMM and GMM require more iteration cycles to converge. RMM costs 19 iteration cycles when $K = 1$ and around 10 iteration cycles in most scenarios. If recall the intuitive results shown in Fig.3, it can be easily noticed that GMM is usually mis-converged to local optimal results. Consequently, the iteration cycles are only with mathematical meaning. Moreover, it is interesting that this mis-converged result is the main reason of the large estimation error. But even with this mis-converged result, the GMM algorithm costs more iteration cycles around 30 and as high as 56. The peak around $K = 4$ may due to the similar reason of QPSK scenario. These results demonstrate that the proposed RMM algorithm not only provides the best accuracy (as DA-all can only be assumed as a rough lower bound), but also affordable deploy cost.

B. FIELD RESULTS

In this subsection, the proposed algorithm will be evaluated with field experiments in a real-life industrial site. In the experiments, two NI USRP-2922 SDR transceiver platforms with omni-directional antennas have been deployed to form a fixed wireless link, which enable the utilization of the baseband I/Q stream. The transmitted signals are configured with QPSK modulation with carrier frequency of 2.4GHz and 915MHz. The frame length has been set to 5*ms*, but without

inter-packet guard time to be equivalent to the continuously sampling of the channel. As a result, each estimation is based on the per frame manner. The configuration of 'QPSK' and '5*ms*' is employed to be similar with the popular IEEE 802.15.4 wireless transceivers utilized in industry applications [26]. However, due the storage speed limitation of hard-disk, the number of per frame have been decreased to enable full recordation. Similar as the numerical experiments, all the received I/Q streams have been recorded and processed in an off-line mode, i.e., processed by the same four estimation algorithms implemented in Matlab. In the DA-all method, all the received I/Q stream will be self-cancelled with known transmitted symbols. Similarly, in the DA-pilot method, the first 1% symbols are assumed with known symbol information, e.g. the preamble utilized in IEEE 802.15.4. The GMM and RMM methods are deployed with no known symbol information. The estimated s and σ of each frame in the selected scenarios have been provided in Fig.9, where the estimated s are shown in the dot lines and the estimated σ are shown in the solid lines.

Most field measurements were obtained in a rolling mill of the state key lab of Rolling and Automation, Northeastern University, Shenyang, China, which is around $300 \times 20 \times 10$ meters large, with a big gantry crane near the roof. In the experiment, a logistical vehicle and operators were asked to work around the transmission link to emulate four typical
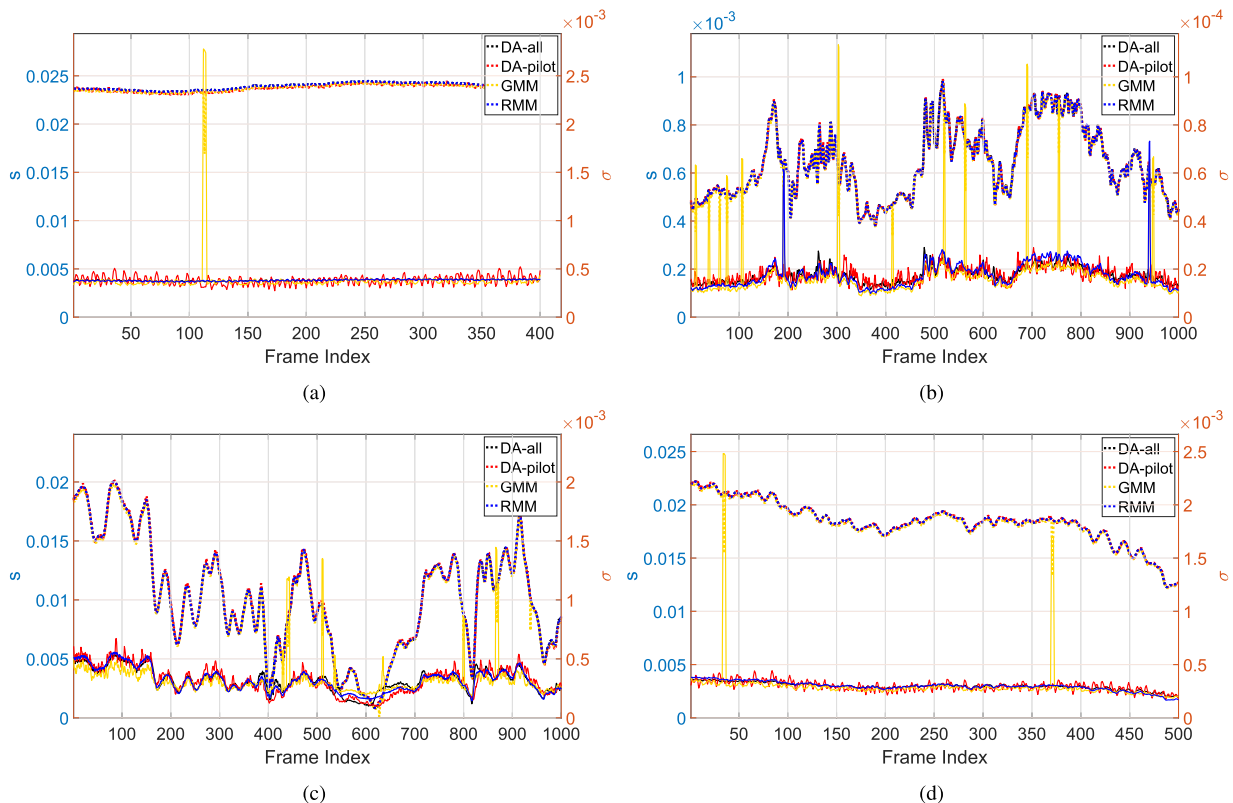

FIGURE 9. The results from field experiment: (a) strict LoS working scenario without nearby moving reflectors; (b) normal LoS working scenario; (c) LoS scenario with nearby logistic vehicle; (d) LoS scenario with nearby operators.

industrial working scenarios. In general, four scenarios have been employed to evaluate the proposed algorithm:

The results shown in Fig.9 (a) are from strict LoS working scenario without any nearby moving reflectors, which lead to the almost static s shown with the dot lines in the upper area and σ shown with the solid lines in the lower area. As there is no ground truth in the field experiment, the similarity with DA-all results can be roughly employed to evaluate the performance of DA-pilot, GMM, and RMM. It is clear that all algorithms show good fitting performance with s, while strong jitters can be noticed in the estimated σ with DA-pilot method and GMM method. The high peak in the GMM estimated σ means a mis-converged estimation occurring in a random pattern. Similar as the numerical experiment shown in section IV.A, the estimated s and σ will be utilized to further calculate K, the qualitative RMSEs of estimated K have been provided in Table 1. As expected, RMM method achieves the best RMSE of 104.8260, while GMM and DA-pilot achieve 428.0779 and 998.7046 respectively. The performance rank of DA-pilot is slightly different with numerical results shown in section IV.A, which may due to the decreased pilot samples in the field experiments(i.e., same 1% pilot ratio with less samples per frame in the field experiments). This can also be inferred from the higher jitter in Fig.9 (a).

TABLE 1. The RMSE of K of evaluated algorithms in typical scenarios.

	direct	LoS	vehicle	operator
DA-pilot	998.7046	376.1614	251.4746	886.1513
GMM	428.0779	264.9381	237.5179	461.5084
RMM	**104.8260**	**187.7393**	**70.1969**	**230.3929**

The results shown in Fig.9 (b) are from the LoS scenario with normal working rolling mill, i.e., the product line was in the working state with running components as well as moving crane, vehicles and operators. As a result, the temporal fading effect with both varying s and σ can be noticed. The estimation performances with this varying scenario are still satisfied, except more mis-converge events occurred, i.e., 12 times for GMM method and 2 times for RMM method. Still, RMM shows the best performance with RMSE of 187.7393, while the RMSEs for GMM and DA-pilot are 264.9381 and 376.1614 respectively.

The results shown in Fig.9 (c) are from the LoS scenario with a logistical vehicle moving around acting as a strong reflector. As this vehicle was asked to moving close to the transmission pair, the deep fading effects can be noticed, where all estimation method show biased estimation in σ around frame index of 600. The proposed RMM method still shows the best performance in this challenge scenario, i.e. the RMSE of 70.1969, while 237.5179 for GMM method and 251.4746 for DA-pilot method.

The results shown in Fig.9 (d) are from the LoS scenario with one operator passing by the transmission pair. Due to the slow speed and low reflection ratio, this scenario shows an almost continuously decreasing pattern. Similar

as previous three scenarios, the RMM method achieves the best performance with 230.3929 RMSE while GMM method achieves 461.5084 RMSE and DA-pilot method achieves 886.1513 RMSE.

Without any doubt, the RMM method shows the closest performances with DA-all in all four scenarios as well as the best qualitative RMSE results, which demonstrate its applicable in different channel scenarios. The GMM and DA-pilot algorithm show not only bias but also high jitter in all four scenarios, which may lead to significant mis-understanding of the link quality. It may also worth to mention that the common iteration number for GMM in the experiments is 5 while 2 for RMM. Without any doubt, these field experiments further validate the efficiency of proposed RMM to enable its wider application.

V. CONCLUSION AND FUTURE WORKS

This paper has proposed a novel general method to estimate the Rician K factor without data-aid requirement. The problem was characterized as a GMM estimation with *a priori* information of modulation scheme. Then the DoFs in GMM estimation has been significantly decreased from $7M$ to 3, i.e. the fading can only affect the scale of specular component s, the variation σ, and the rotation ϕ_0. Consequently, the EM algorithm to estimate GMM parameters was modified to approach the optimized gradient search. Based on this understanding, the 3 DoFs GMM can be further formulated as an RMM based algorithm. Both numerical experiment and field experiment demonstrated the near optimal accuracy of the proposed algorithm with affordable computation cost.

It worths to note that, although this work was designed for the temporal fading channel, the principle of the proposed algorithm can be straightforwardly extended to more general scenarios with the modification of Doppler effect to the phase item following the similar derivation shown in [21]. The proposed algorithm can also be further incorporated with Kalman filter or similar algorithms like in [9] to obtain a predictive link quality estimator for wireless link in the temporal fading environment, which has been believed to be able to further promote the application of wireless industrial networks and other similar applications.

REFERENCES

[1] T. S. Rappaport and C. D. McGillem, "UHF fading in factories," *IEEE J. Sel. Areas Commun.*, vol. 7, no. 1, pp. 40–48, Jan. 1989.

[2] H. Hashemi, M. McGuire, T. Vlasschaert, and D. Tholl, "Measurements and modeling of temporal variations of the indoor radio propagation channel," *IEEE Trans. Veh. Technol.*, vol. 43, no. 3, pp. 733–737, Aug. 1994.

[3] E. Tanghe *et al.*, "The industrial indoor channel: Large-scale and temporal fading at 900, 2400, and 5200 MHz," *IEEE Trans. Wireless Commun.*, vol. 7, no. 7, pp. 2740–2751, Jul. 2008.

[4] P. Agrawal, A. Ahlén, T. Olofsson, and M. Gidlund, "Long term channel characterization for energy efficient transmission in industrial environments," *IEEE Trans. Commun.*, vol. 62, no. 8, pp. 3004–3014, Aug. 2014.

[5] E. Vinogradov, W. Joseph, and C. Oestges, "Measurement-based modeling of time-variant fading statistics in indoor peer-to-peer scenarios," *IEEE Trans. Antenna Propag.*, vol. 63, no. 5, pp. 2252–2263, May 2015.

[6] M. Cheffena, "Propagation channel characteristics of industrial wireless sensor networks [Wireless Corner]," *IEEE Antennas Propag. Mag.*, vol. 58, no. 1, pp. 66–73, Feb. 2016.

[7] M. Eriksson and T. Olofsson, "On long-term statistical dependences in channel gains for fixed wireless links in factories," *IEEE Trans. Commun.*, vol. 64, no. 7, pp. 3078–3091, Jul. 2016.

[8] X. Wu *et al.*, "60-GHz millimeter-wave channel measurements and modeling for indoor office environments," *IEEE Trans. Antennas Propag.*, vol. 65, no. 4, pp. 1912–1924, Apr. 2017.

[9] F. Qin, Q. Zhang, W. Zhang, Y. Yang, J. Ding, and X. Dai, "Link quality estimation in industrial temporal fading channel with augmented Kalman filter," *IEEE Trans. Ind. Informat.*, vol. 15, no. 4, pp. 1936–1946, Apr. 2019.

[10] M. Luvisotto, Z. Pang, and D. Dzung, "Ultra high performance wireless control for critical applications: Challenges and directions," *IEEE Trans. Ind. Inform.*, vol. 13, no. 3, pp. 1448–1459, Jun. 2017.

[11] C. Lu *et al.*, "Real-time wireless sensor-actuator networks for industrial cyber-physical systems," *Proc. IEEE*, vol. 104, no. 5, pp. 1013–1024, May 2016.

[12] X. Dai and Z. Gao, "From model, signal to knowledge: A data-driven perspective of fault detection and diagnosis," *IEEE Trans. Ind. Informat.*, vol. 9, no. 4, pp. 2226–2238, Nov. 2013.

[13] Y. Huang, T. Li, X. Dai, H. Wang, and Y. Yang, "TS2: A realistic IEEE1588 time-synchronization simulator for mobile wireless sensor networks," *Simulation*, vol. 91, no. 2, pp. 164–180, Feb. 2015.

[14] N. Baccour *et al.*, "Radio link quality estimation in wireless sensor networks: A survey," *ACM Trans. Sensor Netw.*, vol. 8, no. 4, Sep. 2012, Art. no. 34.

[15] H. Zhang, L. Sang, and A. Arora, "Comparison of data-driven link estimation methods in low-power wireless networks," *IEEE Trans. Mobile Comput.*, vol. 9, no. 11, pp. 1634–1648, Nov. 2010.

[16] C. G. Koay and P. J. Basser, "Analytically exact correction scheme for signal extraction from noisy magnitude MR signals," *J. Magn. Reson.*, vol. 179, no. 2, pp. 317–322, Apr. 2006.

[17] G. Stuber, *Principles of Mobile Communication*, 3rd ed. New York, NY, USA: Springer, 2012.

[18] R. Bhattacharjea, G. D. Durgin, and C. R. Anderson, "Estimation of Rician K-factors from Block-averaged channel measurements," *IEEE Trans. Wireless Commun.*, vol. 11, no. 12, pp. 4231–4236, Dec. 2012.

[19] C. Tepedelenlioglu, A. Abdi, and G. B. Giannakis, "The Ricean K factor: Estimation and performance analysis," *IEEE Trans. Wireless Commun.*, vol. 2, no. 4, pp. 799–810, Jul. 2003.

[20] Y. Chen and N. C. Beaulieu, "Maximum likelihood estimation of the K factor in Ricean fading channels," *IEEE Commun. Lett.*, vol. 9, no. 12, pp. 1040–1042, Dec. 2005.

[21] K. E. Baddour and T. J. Willink, "Improved estimation of the ricean K-factor from I/Q fading channel samples," *IEEE Trans. Wireless Commun.*, vol. 7, no. 12, pp. 5051–5057, Dec. 2008.

[22] Y. Chen and N. C. Beaulieu, "Estimation of Ricean K parameter and local average SNR from noisy correlated channel samples," *IEEE Trans. Wireless Commun.*, vol. 6, no. 2, pp. 640–648, Feb. 2007.

[23] I. Bousnina, M. B. B. Salah, A. Samet, and I. Dayoub, "Ricean K-Factor and SNR Estimation for M-PSK Modulated Signals Using the Fourth-Order Cross-Moments Matrix," *IEEE Commun. Lett.*, vol. 16, no. 8, pp. 1236–1239, Aug. 2012.

[24] M. B. B. Salah and A. Samet, "Moment-Based joint estimation of Ricean K-factor and SNR over linearly-modulated wireless SIMO channels," *Wireless Pers. Commun.*, vol. 91, no. 2, pp. 903–918, Nov. 2016.

[25] *AT86RF215 Datasheet*, Microchip, Chandler, AZ, USA, 2016.

[26] *CC2420 Datasheet*, Texas Instruments, Dallas, TX, USA, 2008.

QILONG ZHANG received the master's degree in software engineering from the Institute of Computing Technology, Chinese Academy of Sciences, Beijing, China, in 2014. He is currently pursuing the Ph.D. degree with the School of Electronic and Electrical Communication Engineering, University of Chinese Academy of Sciences, Beijing.

His current research interests include the joint optimization method of wireless networks and information systems for industrial applications.

GUOBAO LU (S'18) received the bachelor's degree in electronic science and technology from Tianjin Polytechnic University, Tianjin, China, in 2016. He is currently pursuing the master's degree with the School of Electronic and Electrical Communication Engineering, University of Chinese Academy of Sciences, Beijing.

His current research interest includes the intelligent estimation of industrial wireless channel.

WUXIONG ZHANG (M'13) received the bachelor's degree in information security from Shanghai Jiao Tong University, Shanghai, China, in 2008, and the Ph.D. degree in communication and information systems from the Chinese Academy of Sciences, Beijing, China, in 2013.

He was with a short-term academic exchange to Heriot-Watt University, Edinburgh, U.K., in 2011. He is currently an Associate Professor with the Shanghai Institute of Microsystem and Information Technology, Chinese Academy of Sciences, Shanghai. He has presided/participated in many important research projects in China, including projects funded by the National Natural Science Foundation of China, the National Science and Technology major projects, and the projects funded by the Shanghai Municipal Science and Technology Commission. He has authored or co-authored more than 40 academic papers. His research interests include 5G mobile communication technologies, vehicular networks, and heterogeneous networks.

Dr. Zhang was awarded by the China Communications Society, in 2015, for his contribution in energy-efficient communication and networking.

FEI SHEN (M'14) received the B.Eng. degree in information engineering from Southeast University, China, the M.Sc. degree in communications technology from Ulm University, and the Ph.D. degree from Technische Universit Dresden (TUD), Germany.

She was a Postdoctoral Researcher with TUD and CentraleSupélec, University of Paris-Saclay, France, from 2014 to 2016, and also a Senior Research Engineer with Télécom ParisTech, France, in 2017. She is currently an Associate Professor with the Shanghai Institute of Microsystem and Information Technology, Chinese Academy of Sciences. Her research interests include resource optimization for wireless communications, and edge and fog computing.
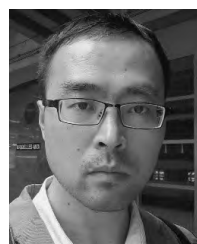
XUEWU DAI (M'09) received the B.Eng. degree in electronic engineering and the M.Sc. degree in computer science from Southwest University, Chongqing, China, in 1999 and 2003, respectively, and the Ph.D. degree from The University of Manchester, U.K., in 2008.

He is currently a Senior Lecturer with the Department of Mathematics, Physics and Electrical Engineering, Northumbria University. His research interests include robust state estimation, networked control systems, wireless sensor actuator networks, and the Industrial Internet of Things.

JIANBIN JIAO (M'10) received the B.S., M.S., and Ph.D. degrees in mechanical and electronic engineering from the Harbin Institute of Technology (HIT), Harbin, China, in 1989, 1992, and 1995, respectively.

From 1997 to 2005, he was an Associate Professor with HIT. Since 2006, he has been a Professor with the School of Electronic, Electrical, and Communication Engineering, University of Chinese Academy of Sciences, Beijing, China. His current research interests include image processing, pattern recognition, and intelligent surveillance.

FEI QIN (S'05–M'12) received the B.Eng. degree in information engineering from the Huazhong University of Science and Technology, Wuhan, China, in 2004, the M.Eng. degree in electronic engineering from the Beijing Institute of Technology, Beijing, China, in 2006, and the Ph.D. degree in electronic and electrical engineering from the University College London, London, U.K., in 2012.

He served as a Product Manager with Crossbow Technology, Beijing Representative Office, from 2006 to 2008. He is currently an Associate Professor with the School of Electronic and Electrical Communication Engineering, University of Chinese Academy of Sciences, Beijing. His current research interests include the joint optimization method of wireless networks and information systems for industrial applications.

• • •